Oncogene (2011) 30, 1470–1480

www.nature.com/onc

ORIGINAL ARTICLE

Transforming growth factor-β regulates the sphere-initiating stem cell-like feature in breast cancer through miRNA-181 and ATM

Y Wang[1,6], Y Yu[1,2,6], A Tsuyada[1,6], X Ren[3], X Wu[4], K Stubblefield[1], EK Rankin-Gee[1] and SE Wang[1,5]

[1]Division of Tumor Cell Biology, Beckman Research Institute of City of Hope, Duarte, CA, USA; [2]Department of Head and Neck Tumor, Tianjin Cancer Institute and Hospital, Tianjin Medical University, Tianjin, China; [3]Department of Immunology and Biotherapy, Tianjin Cancer Institute and Hospital, Tianjin Medical University, Tianjin, China; [4]Bioinformatics Core Facility, City of Hope Comprehensive Cancer Center, Duarte, CA, USA and [5]Cancer Biology Program, City of Hope Comprehensive Cancer Center, Duarte, CA, USA

Recent studies indicate that a subset of cancer cells possessing stem cell properties, referred to as cancer-initiating or cancer stem cells (CSCs), have crucial roles in tumor initiation, metastasis and resistance to anticancer therapies. Transforming growth factor (TGF)-β and their family members have been implicated in both normal (embryonic and somatic) stem cells and CSCs. In this study, we observed that exposure to TGF-β increased the population of breast cancer (BC) cells that can form mammospheres in suspension, a feature endowed by stem cells. This was mediated by the micro (mi)RNA family miR-181, which was upregulated by TGF-β at the post-transcriptional level. Levels of the miR-181 family members were elevated in mammospheres grown in undifferentiating conditions, compared with cells grown in two-dimensional conditions. Ataxia telangiectasia mutated (ATM), a target gene of miR-181, exhibited reduced expression in mammospheres and upon TGF-β treatment. Overexpression of miR-181a/b, or depletion of ATM or its substrate CHK2, was sufficient to induce sphere formation in BC cells. Finally, knockdown of ATM enhanced *in vivo* tumorigenesis of the MDA361 BC cells. Our results elucidate a novel mechanism through which the TGF-β pathway regulates the CSC property by interfering with the tumor suppressor ATM, providing insights into the cellular and environmental factors regulating CSCs, which may guide future studies on therapeutic strategies targeting these cells.
Oncogene (2011) **30,** 1470–1480; doi:10.1038/onc.2010.531; published online 22 November 2010

Keywords: TGF-β; cancer stem cells; microRNA; ATM; CHK2

Correspondence: Dr SE Wang, Division of Tumor Cell Biology, Beckman Research Institute of City of Hope, 1500 East Duarte Road, KCRB Room 2007, Duarte, CA 91010, USA.
E-mail: ewang@coh.org
[6]These authors contributed equally to this work.
Received 14 July 2010; revised 18 October 2010; accepted 19 October 2010; published online 22 November 2010

Introduction

The transforming growth factor-β (TGF-β) ligands are multitasking cytokines that have important roles in embryonic development, cell proliferation, motility and apoptosis, extracellular matrix production and modulation of immune function (Massague, 2008). These ligands signal through the heteromeric complex of transmembrane serine/threonine kinases, the type I and type II receptors (TβRI and TβRII), and activate both the Smad family of transcription factors and non-Smad signaling pathways (Derynck and Zhang, 2003). TGF-β has a dual role in cancer: it limits proliferation in epithelial cells and early-stage cancer cells, whereas in late-stage cancer, it accelerates cancer progression and metastasis (Dumont and Arteaga, 2003; Roberts and Wakefield, 2003). In the cancer niche, TGF-β can be produced and secreted into the extracellular environment by both cancer cells and host cells, such as lymphocytes, macrophages and dendritic cells. In cancer patients, high levels of TGF-β at tumor sites correlate with high histological grade, risk of metastasis, poor response to chemotherapy and poor patient prognosis (Dumont and Arteaga, 2003).

TGF-β signaling has been implicated in cancer stem cells (CSCs), or cancer-initiating cells, which are defined as a subset of cancer cells possessing stem cell properties. CSCs are considered the 'seeds' of cancer for their crucial roles in tumor initiation, metastasis and resistance to anticancer therapies. They resemble embryonic stem cells and somatic (adult) stem cells by their abilities to self-renew and to undergo multilineage differentiation. Characterization of CSCs has been demonstrated in leukemia and solid tumors of the breast, lung, colon, prostate, pancreas, brain and head and neck (reviewed in (Ailles and Weissman, 2007; Visvader and Lindeman, 2008)). In most of these studies, CSCs are prospectively isolated by immunosorting based on the expression of various stemness or multilineage-related surface markers (Dontu, 2008; Visvader and Lindeman, 2008; Charafe-Jauffret *et al*., 2009). Gene expression profiling suggests that the TGF-β pathway is active in $CD44^+$ breast cancer (BC) cells that are enriched for breast cancer stem cells (BCSCs), where its inhibition induces a

more epithelial phenotype (Shipitsin *et al*., 2007). In addition, the epithelial-mesenchymal transition induced by TGF-β treatment or expression of Snail or Twist increases the number of transformed cells with BCSC properties (Mani *et al*., 2008).

A functional enrichment strategy relying on the characteristics of mammary stem cells (MSCs) to escape anoikis and grow into mammospheres in anchorage-independent conditions has been successfully used to obtain highly enriched and functional MSCs from both normal and cancerous breast tissue, as well as from BC cell lines (Dontu *et al*., 2003). Each of these mammospheres clonally originated from one MSC, typically contains ~300 cells undergone various levels of differentiation, and averagely maintains one sphere-initiating MSC (for self-renewal) and some progenitor cells that can differentiate into both epithelial and myoepithelial lineages in Matrigel (Dontu *et al*., 2003). The sphere-forming efficiency (SFE) is thereby used to assess the number of MSCs in the bulk of normal or cancer cells, and ranges 0.1–0.7% in normal mammary epithelial cells, whereas 1–3% in BC cell lines (Dontu *et al*., 2003; Charafe-Jauffret *et al*., 2009). Genes that are differentially expressed by sphere cells highlight pathways implicated in maintaining the stem cell status (Charafe-Jauffret *et al*., 2009). In this study, we examined the function of TGF-β in regulating the BC population with the sphere-forming CSC feature, and identified a novel micro (mi)RNA-mediated mechanism that targets the ataxia telangiectasia mutated (ATM) tumor suppressive pathway.

Results

Identification of the miR-181 family members as TGF-β target genes

MiRNAs are naturally occurring non-coding small RNA molecules that have crucial functions in cells by base pairing to the 3′ untranslated region (UTR) of target mRNAs, resulting in mRNA degradation or translation inhibition. To explore the role of TGF-β in miRNA regulation, we performed miRNA array analysis in the BC cell line MDA231 and the non-transformed mammary epithelial cells MCF10A. The miRNAs were filtered for expression changes >1.5-fold after 24 h of TGF-β treatment; 13 miRNAs in MDA231 and 11 miRNAs in MCF10A cells were identified (Figure 1a).

a

	ID	+TGF-β	Control	FC	*p* (<0.05)
MDA-231	**hsa-miR-181a***	8.736	8.072	0.664	0.00719
	hsa-miR-181a-2*	7.342	5.636	1.706	1.00E-05
	hsa-miR-181b	9.228	8.582	0.646	0.00506
	hsa-miR-193b	8.141	7.427	0.715	0.00318
	hsa-miR-200b	5.629	4.451	1.178	1.00E-04
	hsa-miR-21*	10.597	8.81	1.787	0.00076
	hsa-miR-27a	14.181	13.287	0.894	0.01061
	hsa-miR-455-3p	8.715	8.036	0.678	0.0021
	hsa-miR-455-5p	6.21	4.9	1.309	0.01851
	hsa-miR-582-5p	5.897	5.259	0.638	0.01059
	hsa-miR-598	5.609	6.367	-0.758	0.00116
	hsa-miR-769-5p	5.338	5.954	-0.616	0.04449
	hsa-miR-886-3p	10.731	11.414	-0.683	0.00804

	ID	+TGF-β	Control	FC	*p* (<0.05)
MCF-10A	**hsa-miR-181a-2***	5.865	5.257	0.609	9.00E-05
	hsa-miR-181d	6.822	4.789	2.033	0.00033
	hsa-miR-197	8.335	6.525	1.81	0.00066
	hsa-miR-21*	9.201	8.292	0.909	0.01781
	hsa-miR-34b	5.306	3.229	2.076	0.00139
	hsa-miR-376a	5.128	3.646	1.482	0.00029
	hsa-miR-376c	5.445	4.327	1.118	2.00E-05
	hsa-miR-378	9.049	9.808	-0.759	0.0109
	hsa-miR-574-3p	8.899	7.158	1.741	0.00041
	hsa-miR-744*	5.91	4.373	1.537	0.00185
	hsa-miR-766	6.253	4.972	1.28	0.00056

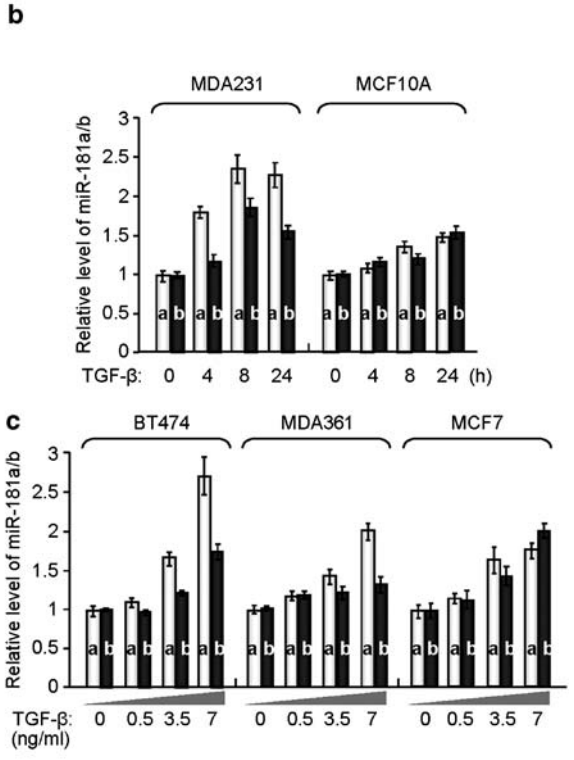

Figure 1 Identification of the miR-181 family as TGF-β target genes. (**a**) MiRNAs altered by TGF-β treatment. Total RNAs were prepared from MDA231 and MCF10A cells treated with TGF-β (2 ng/ml) or vehicle for 24 h in three independent experiments, and subjected to Agilent miRNA microarrays (Agilent Technologies, Inc., Santa Clara, CA, USA). The differentially expressed miRNAs were selected by statistical criteria of >1.5-fold changes (log base 2 = ±0.58) and $P<0.05$ by Student's *t*-test (indicated in log 2 value). Fold change: fold change (in log 2) of TGF-β-treated sample compared with control sample. (**b**) MDA231 and MCF10A cells were treated with TGF-β (2 ng/ml) or vehicle for indicated time. Total RNA was isolated and subjected to qRT–PCR for miR-181a and miR-181b. Data were normalized to the level of U6, and then compared with that in untreated cells, which was set as 1. Each datum point represents the mean ± s.d. of three wells. (**c**) BC cell lines BT474, MDA361 and MCF7 were treated with TGF-β at the indicated final concentrations or vehicle for 72 h. Total RNA was isolated and subjected to qRT–PCR for miR-181a and miR-181b.

Predicted target genes of these miRNAs were analyzed using TargetScanHuman 5.1 (Supplementary Table 1). Genes that were common to both cell lines were selected and mapped to their corresponding gene networks by Ingenuity Pathways analysis (IPA 8.6, Ingenuity Systems, Inc., Redwood City, CA, USA) (Supplementary Figure S1 and Supplementary Table 2).

It was noticed that members of the miR-181 family were upregulated by TGF-β in both cell lines (Figure 1a). This miRNA family includes the guiding strands miR-181a/b/c/d that share the same seed sequence, and the passenger strands miR-181a*and miR-181a-2*that are present at lower abundances. It has been reported that miR-181 family members have an important role in hepatic CSCs by targeting hepatic transcriptional regulators of differentiation (Ji *et al*., 2009). Elevated levels of miR-181 are observed in the cancer of breast, prostate and pancreas (Volinia *et al*., 2006). We thereby focused on the miR-181 family in this study, for their potential function in BCSCs as the downstream effectors of TGF-β signaling. Quantitative reverse transcriptase (qRT)–PCR confirmed that TGF-β induced the expression of miR-181a and miR-181b in both MDA231 and MCF10A cells (Figure 1b). A dose-dependent induction was also observed in other three BC cell lines, BT474, MDA361 and MCF7 (Figure 1c).

The context-dependent effect of TGF-β on the sphere-initiating CSC-like feature

An *in vitro* cultivation system that allows propagation of human mammary epithelial cells and BC cells in an undifferentiated state, based on their ability to proliferate in suspension as non-adherent mammospheres, has been established and used in several recent reports (Dontu *et al*., 2003; Mani *et al*., 2008; Cicalese *et al*., 2009; Pece *et al*., 2010). Using this approach, we examined the SFE in a panel of BC cell lines. Because MDA231 and MCF10A cells could not form mammospheres using this system, three BC cell lines that could, that is, BT474, MDA361 and MCF7, were selected for further investigation. All three cell lines exhibited SFE of 1–3%, which is consistent with the reported CSC populations in primary human cancers (Figure 2a). The spheres formed from these cell lines also exhibited the typical size reported in others' studies, and expressed the stem cell markers Oct4 and Nanog (Figure 2b). Immunofluorescence assay further indicated that the spheres but not parental cells grown in two dimension (2D) contained a small number of cells expressing cytokeratin 5, a marker of MSCs (Figure 2c). The majority of the sphere cells expressed cytokeratin 8/18, markers of differentiated cells, suggesting the heterogeneity of spheres formed from BC cell lines (Figure 2c). When cells were pretreated with TGF-β for 3 days, the SFE of BT474 and MDA361 cells was significantly induced in a dose-dependent manner, whereas in MCF7, TGF-β decreased the SFE (Figure 2d). These results suggest a context-dependent mechanism in the regulation of CSCs by TGF-β. As both BT474 and MDA361 cells naturally overexpress HER2, whereas MCF7 cells are $ER^+/PR^+/HER2^-$, we examined if overexpression of HER2 affected the effect of TGF-β on MCF7 sphere formation. HER2-transduced MCF7 cells (MCF7/HER2) were generated, and the overexpression and phosphorylation/activation of HER2 were confirmed by western blot. However, similar to the control MCF7 cells, the SFE of MCF7/HER2 cells was also decreased by TGF-β (Supplementary Figure S2), indicating that other factors in BT474 and MDA361 cells are responsible for the context-dependent function of TGF-β.

MiR-181 regulates sphere formation

The reported function of miR-181 in hepatic CSCs urged us to examine its role in regulating BCSCs. Levels of the miR-181 family members were elevated in sphere cells by two–fourfold, compared with the parental BT474, MDA361 and MCF7 cells grown in 2D; their expression levels were reduced when sphere cells were dissociated and replated to grow in 2D (Figure 3a). This is unlikely to be an effect of the medium used in mammosphere culture, as the same medium and culture condition did not induce miR-181 expression in the MDA231 BC cells, which could not form mammospheres (Supplementary Figure S3). A hairpin inhibitor of miR-181a that efficiently inhibited miR-181a and partially inhibited miR-181b reduced both basal and TGF-β-induced SFE in BT474 and MDA361 cells, but had no effect in MCF7 cells (Figure 3b). When a plasmid carrying the miR-181a/b gene cluster in chromosome 1 was transfected into the cells to overexpress miR-181, increased SFE was observed in both transfected BT474 and MDA361 cells, but not in MCF7 cells (Figure 3c). Notably, the overexpression levels of miR-181a/b in plasmid-transfected cells were comparable to those in TGF-β-treated cells (Figure 1c), and were sufficient to significantly induce sphere formation in both BT474 and MDA361 cells (Figure 3c, top panels). Therefore, although the induction of miR-181 by TGF-β was modest (1.5–2.5 folds), it seems to be sufficient to exert an effect on sphere formation. These data also suggest that TGF-β induces sphere formation through upregulating miR-181, which induces this stem cell phenotype in a context-dependent manner that requires certain factor(s) or functional link(s) present in BT474 and MDA361, but not MCF7 cells. We also compared levels of several previously reported cancer-related miRNAs in sphere cells and 2D-cultured parental cells. MiR-21 was also elevated in the spheres of BT474 and MDA361 cells (Supplementary Figure S4). However, a miR-21 hairpin inhibitor did not affect SFE as potently as the miR-181a inhibitor, when transfected alone or in combination with the miR-181a inhibitor (Figure 3d).

TGF-β induces miR-181a/b at the post-transcriptional level

Two distinct mechanisms have been reported in the regulation of miRNAs by TGF-β. The TGF-β down-

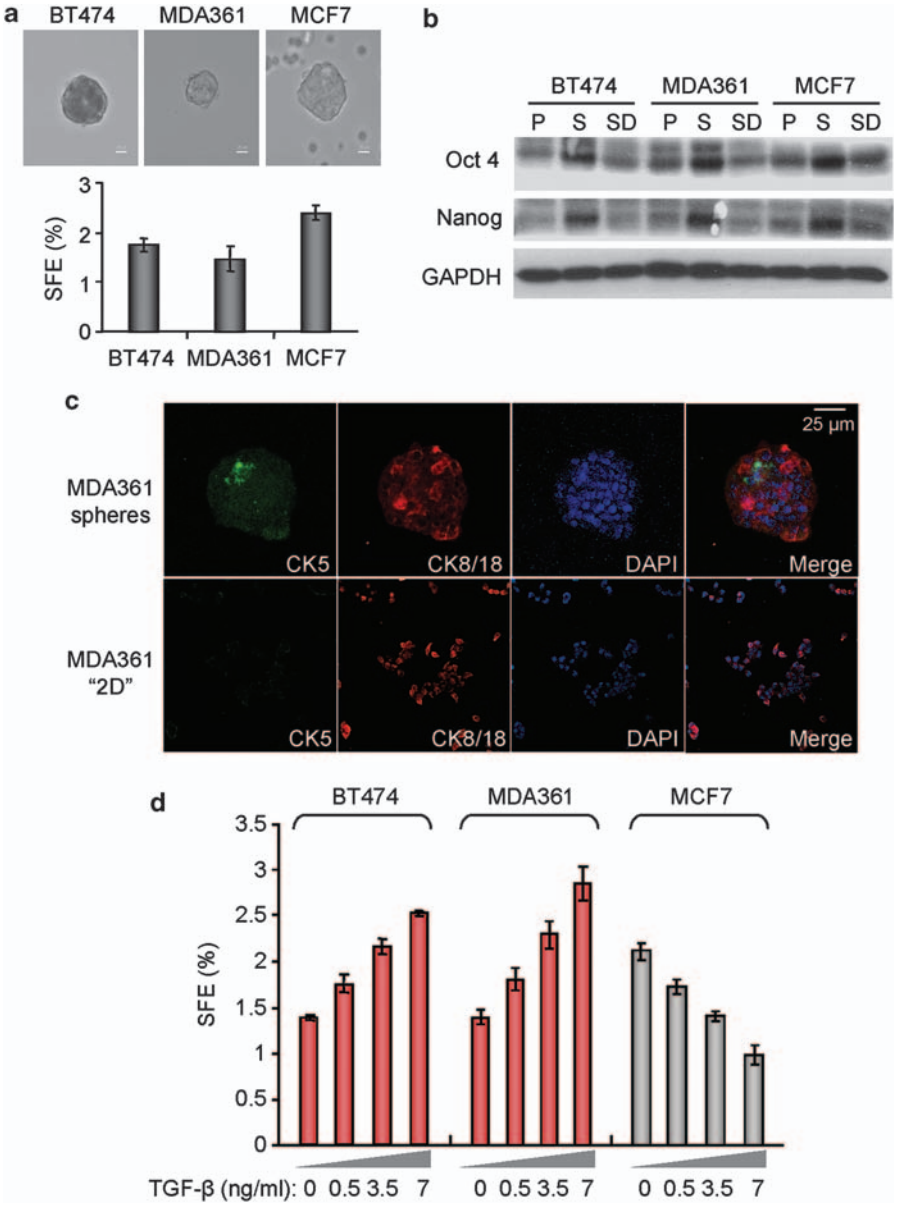

Figure 2 The context-dependent effect of TGF-β on the sphere-initiating CSC-like feature. (**a**) BC cell lines BT474, MDA361 and MCF7 contained a small cell population that could initiate spheres when cultured in suspension. Single cells were plated in ultralow attachment plates as described in Materials and methods section, so that cells with stem cell properties were allowed to grow as non-adherent spheroids (mammospheres). Images of the mammospheres were captured on day 7. Numbers of the mammospheres (diameter $\geqslant 70\,\mu m$) were counted, and the SFE was calculated based on the numbers of cells that were initially seeded. Each data represents the mean ± s.d. of three wells. Bars equal 25 μm. (**b**) Protein extracts were prepared from the parental (P) cells growing in 2D, 7-day sphere (S) cells, and cells that were dissociated from 7-day spheres and subsequently cultured in 2D-differentiating condition (s.d.). Western blot was performed using indicated antibodies. Glyceraldehyde 3-phosphate dehydrogenase was used as a loading control. (**c**) Immunofluorescence assay images of MDA361 spheres and 2D-cultured cells stained with antibodies against cytokeratin 5 (green) and cytokeratin 8/18 (red). Stain 4′,6-Diamidino-2-phenylindole: nuclei staining. The bar equals 25 μm. (**d**) Cells grown in 2D were treated with TGF-β at the indicated concentrations for 72 h, before being harvested for sphere formation assay in the absence of TGF-β. Spheres were counted on day 7 and SFE was calculated.

stream effectors Smads are reported to bind to and activate the promoter of miR-155 (Kong *et al*., 2008). Whereas in the regulation of miR-21, Smad2/3 bind to the primary transcript of miR-21 through interacting with the Drosha miRNA processing complex, which facilitates miR-21 maturation (Davis *et al*., 2008). To investigate which mechanism is involved in the regulation of miR-181, we examined levels of the primary (pri-) miR-181a-1 and the precursor miR-181a-1 in TGF-β-treated cells by qRT–PCR. Although TGF-β induced the mature forms of miR-181 (Figure 1c), it decreased their primary and precursor forms in all four cell lines tested (Figure 4a), suggesting the regulation occurs at the level of miRNA maturation. It has been reported that MDA231 cells do

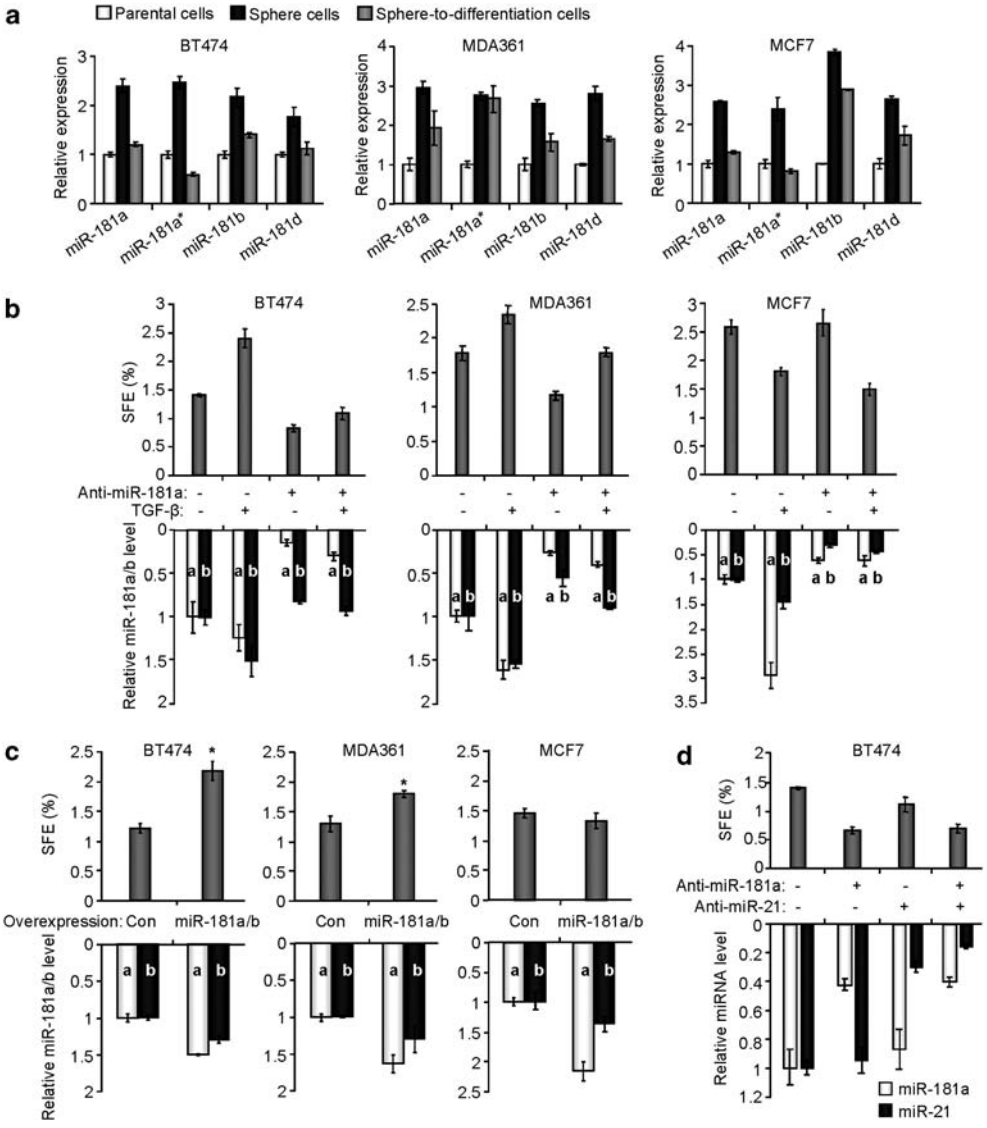

Figure 3 MiR-181 regulates sphere formation. (**a**) Total RNA was isolated from parental cells, sphere cells and sphere-to-differentiation cells as described in Figure 2b, and subjected to qRT–PCR for miR-181a, miR-181a*, miR-181b and miR-181d. Data were normalized to the level of U6 and then compared with that in parental cells, which was set as 1. (**b**) Cells grown in 2D were transiently transfected with miR-181a hairpin inhibitor or a control reagent. TGF-β (3.5 ng/ml) or vehicle was added at 6 h after transfection. After 72 h, cells were harvested; half were used for RNA extraction and qRT–PCR of miR-181a/b (bottom), and half for sphere formation assay (top). SFE was assessed on day 7. (**c**) Cells grown in 2D were transiently transfected with a miR-181a/b expression plasmid or the vector control. At 72 h after transfection, cells were analyzed for the levels of miR-181a/b by qRT–PCR (bottom) and for SFE (top). $^*P<0.005$. (**d**) BT474 cells grown in 2D were transiently transfected with the hairpin inhibitors of miR-181a or miR-21, either alone or in combination at equal amount. At 72 h after transfection, cells were analyzed for the levels of miR-181a and miR-21 by qRT–PCR (bottom) and for SFE (top).

not undergo Smad4 translocation into the nucleus in response to TGF-β stimulation (Ren *et al*., 2009). In these cells, decreased pri- and precursor miR-181a-1 levels and increased mature miR-181 levels were still observed (Figures 1b and 4a), consistent with the reported observation that the Smad2/3-Drosha interaction is Smad4-independent (Davis *et al*., 2008). In RNA immunoprecipitation-coupled RT–PCR, pri-miR-181a-1, but not the mature miR-181a, was detected in the precipitates of Smad2/3 and Drosha, but not immunoglobulin (Ig)G, in a TGF-β-inducible manner (Figure 4b), suggesting that similar to the regulation of miR-21, TGF-β induces binding of Smad2/3 to the primary transcripts of miR-181 and regulates their maturation. Smad4 knockdown using small interfering (si)RNA did not interfere, but instead increased miR-181 levels and SFE (Figure 4c), suggesting that lower levels of Smad4 may contribute to a switch of Smad2/3 function from Smad4-mediated transcriptional regulation to Drosha-mediated miRNA maturation.

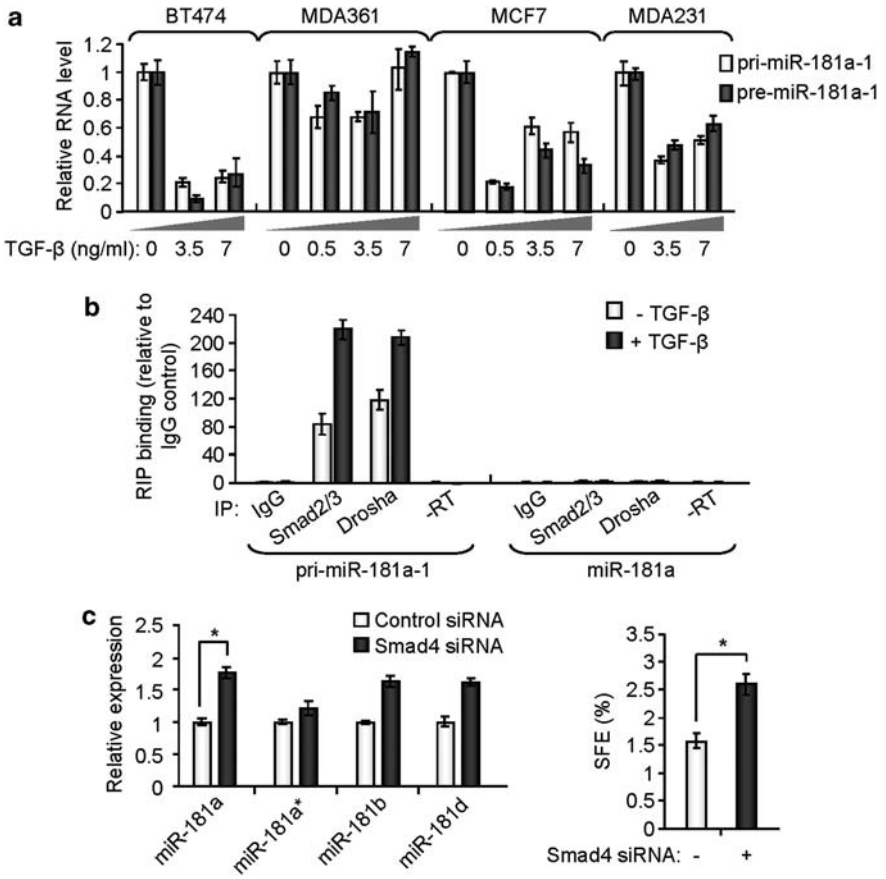

Figure 4 TGF-β induces miR-181a/b at the post-transcriptional level. (**a**) The qRT–PCR of the pri-miR-181a-1 and the precursor miR-181a-1 in cells treated with TGF-β at the indicated concentrations for 72 h. Data were normalized to glyceraldehyde 3-phosphate dehydrogenase in each sample and compared with that of untreated cells, which was set as 1. (**b**) RNA immunoprecipitation (RIP) was carried out in BT474 cells treated with TGF-β (3.5 ng/ml) or vehicle for 24 h. Antibodies against Smad2/3, Drosha or IgG (as a negative control) was used in the immunoprecipitation as described in the Materials and methods section. The qRT–PCR of pri-miR-181a-1 and the mature miR-181a were performed, using the precursor RIP RNA sample without reverse transcription reaction (−RT) as a negative control. Data were compared with the control RIP sample with IgG. (**c**) BT474 cells grown in 2D were transiently transfected with siRNA-targeting Smad4 or control siRNA. After 72 h, cells were analyzed for the levels of miR-181a/a*/b/d by qRT–PCR (left) and for SFE (right). $*P<0.005$.

ATM, a miR-181 target, suppresses sphere formation through phosphorylating CHK2

One of the predicted miR-181 target gene is ATM, a serine/threonine kinase that functions as a tumor suppressor. In the function annotations of the predicted target genes of TGF-β-regulated miRNAs (Supplementary Figure S1), ATM appeared in 11 out of the 12 top ranked functional networks (Supplementary Table 2). To determine if ATM is a real target of miR-181, we first interrogated the 3′UTR sequence of human ATM gene transcript using TargetScanHuman 5.1 (www.targetscan.org) and miRDB (www.mirdb.org). Two potential miR-181a/b/c/d-targeting sites, at the positions 123 and 3525 in the ATM 3′UTR, were identified (Figure 5a). We then cloned these two putative miR-181 binding regions, either together or individually, downstream to a luciferase reporter gene in psiCHECK vector (Promega Corporation, Madison, WI, USA), and transfected 293 cells with these constructs or a control vector containing a scrambled sequence. Co-transfection with the plasmid expressing miR-181a/b efficiently suppressed expression of the luciferase reporter followed by either putative miR-181 binding site, but not the scrambled sequence; the reporter construct containing both miR-181 binding sites showed the strongest inhibition by miR-181a/b (Figure 5b). Consistently, TGF-β also suppressed these ATM 3′UTR reporters containing one or two miR-181 binding sites (Figure 5b). Suppression of the ATM 3′UTR reporter by overexpressed miR-181a/b and TGF-β treatment was also observed in transfected BT474, MDA361 and MCF7 cells (Figure 5c).

The levels of ATM significantly reduced in the spheres formed by all three BC cell lines (Figure 5d), which was consistent with the elevated miR-181 levels in the spheres (Figure 3a). The miR-181a inhibitor increased basal ATM expression and abolished the suppressive effect of TGF-β on ATM, whereas miR-181a/b overexpression decreased ATM protein level (Figure 5e). Treatment with TGF-β, which induced miR-181, reduced the mRNA levels of ATM in BT474 and MCF7, but not significantly in MDA361 (Figure 5f). Nonetheless, at the protein level, ATM was significantly

suppressed by TGF-β in all three cell lines (Figure 5g). Similar to the pattern of cell line-specific regulation by TGF-β, knockdown of ATM by siRNA significantly increased SFE in BT474 and MDA361, but not MCF7 cells (Figure 5h). These results indicate that the distinct effect of TGF-β and miR-181 in different cell lines is due to a context-dependent function of ATM.

ATM is an important cell cycle checkpoint kinase that phosphorylates a wide variety of substrates, including p53, BRCA1 and CHK2 (Kastan and Lim, 2000). To further identify which ATM downstream effector is involved in the regulation of sphere formation, we individually knocked down the expression of p53, BRCA1 and CHK2 using siRNAs. Knockdown of CHK2, but not the other two genes, induced SFE in all three cell lines tested (Figure 5h). Reduced CHK2 phosphorylation, as a result of the reduced ATM levels, was observed in the spheres formed by all three cell lines, compared with the cells grown under regular culture conditions (Figure 5d). This suggests that the ATM

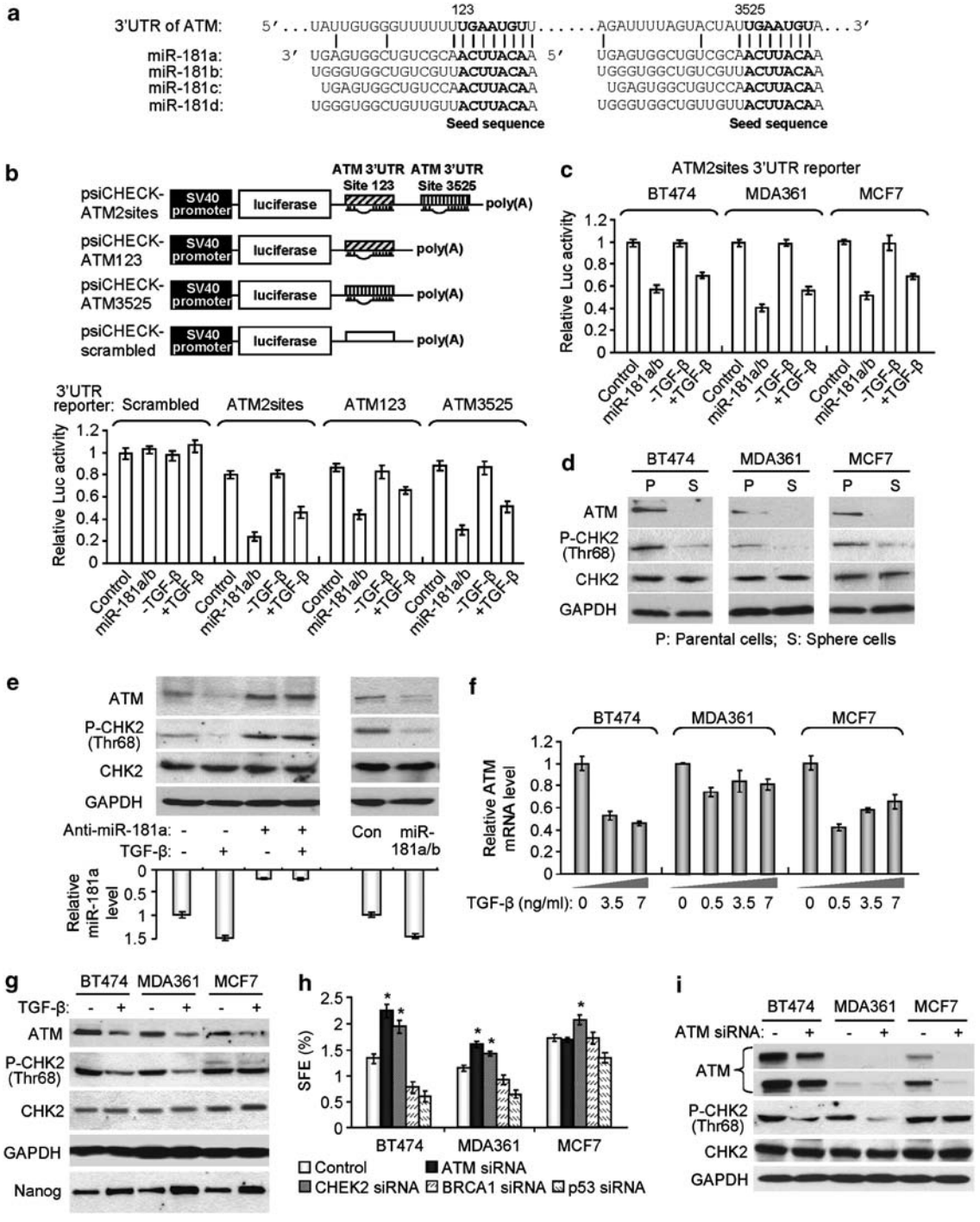

effector CHK2 functions as a suppressor of sphere formation. Western blot further indicated that treatment with TGF-β, overexpression of miR-181a/b or transfection of ATM siRNA all reduced CHK2 phosphorylation at Thr68, a reported ATM phosphorylation site (Kastan and Lim, 2000), in BT474 and MDA361, but not MCF7 cells (Figures 5e, g and i). These results further suggest that in BT474 and MDA361 cells, ATM negatively regulates sphere formation via activating CHK2, which may be controlled by another kinase in MCF7 cells.

Knockdown of ATM enhances the in vivo *tumorigenesis of BC cells*

To further examine the role of ATM in tumorigenesis, we constructed MDA361 cells stably expressing doxycycline (Dox)-inducible ATM short hairpin RNA. Treatment with Dox efficiently decreased the protein level of ATM (Figure 6a) and induced sphere formation (Figure 6b). When 5×10^5 cells were injected into the mammary fat pads of immunocompromised mice, three out of five mice treated with Dox formed tumors within 3 weeks, whereas no tumor was developed in the control group (−Dox; $n = 5$) (Figure 6c).

Discussion

Similar to embryonic and somatic stem cells, the self-renewal and differentiation of CSCs are simultaneously regulated by intrinsic (cancer cell endowed) and extrinsic (microenvironmental) factors. Here we reported that TGF-β, a cytokine whose level is often elevated in the tumor microenvironment and associated with advanced BCs, stimulated the signature phenotype of CSCs to proliferate in suspension as non-adherent mammospheres. This regulation of CSCs by a microenvironmental factor is dependent on certain intrinsic pathways within cancer cells, such as the signaling axis of ATM and CHK2. As a result, CSCs that carry different genetic or epigenetic alterations may respond differently to the same cues in the cancer niche. Other factors in the tumor microenvironment that regulate CSCs, and how CSCs, in turn, modify the cancer niche and regulate their neighbor cells are yet to be identified.

Members of the TGF-β family have been implicated in the development of various organs and the maintenance of embryonic stem cell pluripotency (Topczewska *et al*., 2006; Watabe and Miyazono, 2009). Nodal and activin have been reported to maintain pluripotency of human embryonic stem cells by controlling the expression of Nanog, a critical transcriptional factor for the 'stemness' status, through binding of Smad2/3 to *Nanog* promoter (Vallier *et al*., 2009). In our study, TGF-β

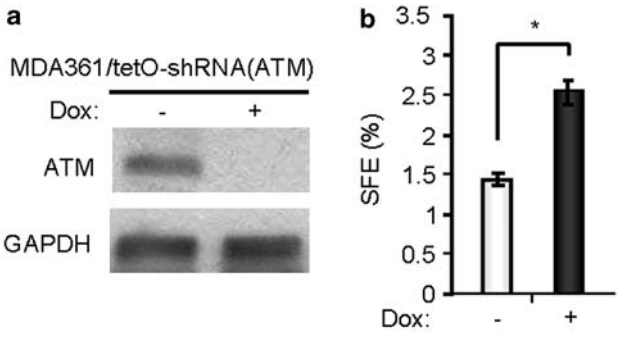

c

In Vivo Tumor Formation (Tumors/Injections)

MDA361/tetO-shRNA(ATM)	
-Dox	+Dox
0/5	3/5

Figure 6 Knockdown of ATM enhances the *in vivo* tumorigenesis of BC cells. **(a)** MDA361/tetO-short hairpin RNA(ATM) cells were treated in the absence or presence of Dox (1 μg/ml) for 48 h and analyzed for ATM expression by western blot. **(b)** The same cells were treated in the absence or presence of Dox for 48 h before analyzed for SFE as described. $^*P < 0.005$. **(c)** NOD/SCID/IL2Rγ-null mice were injected in the no. 4 mammary fat pad with 5×10^5 of MDA361/tetO-short hairpin RNA(ATM) cells, and divided into two groups (five mice per group) for treatment with Dox or control. Tumor formation was indicated by tumors/injections at 3 weeks after injection.

Figure 5 ATM, a miR-181 target, suppresses sphere formation through phosphorylating CHK2. **(a)** The miR-181a/b/c/d-targeting sites in the 3′UTR of ATM mRNA predicted by TargetScanHuman 5.1 (www.targetscan.org) and miRDB (www.mirdb.org). **(b)** The psiCHECK luciferase reporters containing the miR-18- targeting site at 123, the site at 3525 or both sites, or a control reporter containing a scrambled sequence, were used to transfect 293 cells, together with a miR-181a/b-expressing plasmid or vector. For the TGF-β treatment experiments, cells were transfected with each reporter; TGF-β (3.5 ng/ml) or vehicle was added at 24 h after transfection. Luciferase activity was analyzed at 48 h post transfection, and compared with the cells transfected with the control plasmids. **(c)** The luciferase reporter containing both miR-181-targeting sites in ATM 3′UTR was transfected into BT474, MDA361 or MCF7 cells, together with the miR-181a/b-expressing plasmid or vector. For the TGF-β treatment experiments, cells were transfected with the reporter only; TGF-β (3.5 ng/ml) or vehicle was added at 24 h after transfection. Luciferase activity was analyzed at 48 h post transfection, and compared with the cells transfected with the control plasmids. **(d)** Protein extracts of parental (P) and sphere (S) cells were prepared and subjected to western blot analysis. Glyceraldehyde 3-phosphate dehydrogenase (GAPDH) was used as a loading control. **(e)** BT474 cells grown in 2D were transfected with a miR-181a hairpin inhibitor (or control reagent) or a miR-181a/b-expressing plasmid (or vector). TGF-β or vehicle was added at 6 h after transfection. After 72 h, cells were harvested; half were used for RNA extraction and qRT–PCR of miR-181a (bottom), and half for protein extraction and western blot analysis (top). **(f)** Total RNA isolated from cells treated with TGF-β at the indicated concentrations for 72 h was analyzed for ATM mRNA level by qRT–PCR. Data were normalized to GAPDH in each sample and compared with that of untreated cells. **(g)** Cells grown in 2D were treated with TGF-β or vehicle for 72 h before being lysed and subjected to western blot analysis. **(h)** Cells grown in 2D were transiently transfected with siRNA targeting ATM, CHEK2, BRCA1, p53 or control siRNA. At 72 h after transfection, cells were analyzed for SFE as described in Figure 3b. $^*P < 0.005$. **(i)** Western blot of the indicated proteins in cells transfected with ATM siRNA or control siRNA.

treatment induced Nanog expression in all three BC cell lines tested (Figure 5g), whereas the sphere-forming CSC property was only induced in BT474 and MDA361, but not MCF7 cells (Figure 2d). This suggests that increased expression of Nanog is not sufficient to induce the sphere-forming phenotype of CSCs. Instead, knockdown of CHK2 consistently induced sphere formation in all BC cell lines (Figure 5h). Although the role of the miR-181/ATM/CHK2 axis in the regulation of embryonic and somatic stem cells needs to be further investigated, it is likely that in cancer, both induction of Nanog and suppression of CHK2 function through the mechanism identified herein mediate the regulation of CSCs by TGF-β.

It has been reported that levels of the miR-181 family members are elevated in epithelial cell adhesion molecule-positive hepatic CSCs and in embryonic livers (Ji *et al*., 2009). In another study, significant upregulation of miR-181b and miR-181d is observed in the livers of mice during early carcinogenesis (Wang *et al*., 2010). Expression of the tissue inhibitor of metalloprotease 3, another validated target of miR-181, is markedly suppressed in these livers. TGF-β is found to induce miR-181b through a Smad4-dependent mechanism in hepatic cells, as knockdown of Smad4 by siRNA interferes with miR-181b expression in these cells (Wang *et al*., 2010). In contrast, our data indicated that in BC cells, Smad4 knockdown instead increased miR-181 expression and SFE (Figure 4c). The entire miR-181 family is encoded by three genomic loci in chromosomes 1, 9 and 19, and the transcription of these loci is controlled by different promoter regions without sequence homology. Our data herein suggested that at least in BC cells, TGF-β upregulates the entire miR-181 family at the post-transcriptional level through the Smad4-independent functions of Smad2/3, such as their interaction with Drosha. This upregulation simultaneously increases both the guiding strands and the passenger strands. As the passenger strands usually undergo rapid degradation and exist at much lower basal levels compared with the guiding strands, their fold induction by TGF-β treatment seemed to be more significant (miR-181a*and miR-181a-2*, Figure 1a). However, it is also possible that TGF-β has a specific effect on the stability of miR-181a*and miR-181a-2*, resulting in further increases of these passenger strands. Argonaute proteins, the effector molecules in miRNA-mediated RNA interference, are involved in multiple miRNA-related functions, including the incorporation of miRNA into the RNA-induced silencing complex, cleavage of the target mRNA, miRNA maturation and removal of the passenger strand from RNA-induced silencing complex after maturation (Diederichs and Haber, 2007). Whether TGF-β regulates miRNA maturation and the fate of the passenger strands through affecting the function of Argonaute proteins is an interesting direction to further investigate.

In the study by Davis *et al*. (2008), the precursor miR-21 level is increased upon TGF-β treatment, whereas in our study, both pri- and precursor miR-181a-1 levels decreased in TGF-β-treated cells (Figure 4a). Following Drosha-mediated cleavage of the primary transcripts, the miRNA hairpin precursors are further processed by the Dicer RNase and/or Argonaute proteins to generate the mature miRNAs (Diederichs and Haber, 2007). Therefore, the miRNA precursor, as an intermediate during miRNA maturation, only transiently exists and undergoes rapid turnover. As such, the levels of miRNA precursors detected by PCR in TGF-β-treated cells are affected by their turnover time, which may be different for each miRNA regulated through the Smad2/3-Drosha mechanism. Our results further suggest that the level of Smad4 may determine the function of Smad2/3 by altering the equilibrium between Smad4-mediated transcriptional regulation (favored at a high Smad4 level) and Drosha-mediated miRNA maturation (favored at a low Smad4 level). It was recently reported that the tumor suppressor p53 interacts with the Drosha processing complex through the association with DEAD-box RNA helicase p68 (DDX5) and facilitates the processing of primary miRNAs to precursor miRNAs (Suzuki *et al*., 2009). As p53 can interact with Smad2 (Cordenonsi *et al*., 2003), whether p53 has a role in mediating the interaction between Smad2/3 and Drosha needs further investigation, and may reveal a functional link between the p53 and TGF-β pathways in regulating miRNA biogenesis.

A novel miR-181 target, ATM, was identified in this study. ATM is a key regulator of the DNA damage response through phosphorylating a variety of proteins involved in DNA repair, cell cycle regulation and apoptosis (Kastan and Lim, 2000). Consistent with this function, ATM deficient tumors have been shown to be more sensitive to DNA double-strand break-inducing agents (Tribius *et al*., 2001). Small molecule inhibitors of ATM have also been shown to sensitize cancer cells to DNA-damaging drugs, and are proposed to be used as drug-sensitizing agents for anti-cancer chemotherapy. However, a number of studies suggest an opposite effect of ATM mutation/deletion, which correlates with resistance to DNA-damaging chemotherapy and poor patient survival (Haidar *et al*., 2000; Austen *et al*., 2007). Our results indicated that suppression of ATM or CHK2 could induce the sphere-forming CSC phenotype. As CSCs have been implicated in resistance to chemotherapy, it is possible that mutation/deletion of ATM or CHK2, or their downregulation by factors such as TGF-β and miR-181, contributes to drug resistance through regulating the CSC population. Similarly, pharmaceutical inhibition of ATM is unlikely to have a beneficial effect due to its potential influence on CSCs. Further studies are required to evaluate the therapeutic value of TGF-β/miR-181 interventions for their effects on CSCs and drug resistance.

Materials and methods

Cell lines, plasmids and viruses

This information can be found in the Supplementary Materials.

Sphere formation assay
Mammosphere culture was performed as described by (Dontu *et al*. (2003) with slight modifications. Single cells were plated in ultralow attachment plates (Corning, Corning, NY, USA) at a density of 4000 cells per ml in serum-free Dulbecco′s modified Eagle medium/F12 (Invitrogen; Carlsbad, CA, USA) supplemented with 10 ng/ml basic fibroblast growth factor (Sigma-Aldrich, St Louis, MO, USA), 20 ng/ml epidermal growth factor (Invitrogen), 5 μg/ml insulin (Sigma-Aldrich) and 0.4% bovine serum albumin (Sigma-Aldrich). On day 7–9, numbers of the mammospheres (diameter $\geqslant$ 70 μm) were counted, and SFE calculated based on the numbers of initially seeded cells. To ensure that each mammosphere was clonally originated from a single cell, cells grown in the regular 2D conditions were labeled with PKH67 green fluorescent or PKH26 red fluorescent cell linkers (Sigma-Aldrich) following the manufacturer's protocol, and mixed at a 1:1 ratio, before initial seeding for sphere forming culture. After 7–9 days, spheres were monitored under a Nikon Eclipse TE2000-S fluorescent microscope (Nikon, Melville, NY, USA), and $>$95% of the spheres were labeled with a single dye (data not shown). Mammospheres of 7–9 days were collected by gentle centrifugation (320 g), washed with 1 $\times$ phosphate buffered saline, and subjected to RNA or protein preparation (described below). Some mammospheres were enzymatically dissociated by incubation in trypsin-EDTA solution (Invitrogen) for 2 min at 37 °C. Single cell suspensions were then plated in tissue-culture coated plates to allow differentiation under the regular 2D culture conditions. To study the effect of TGF-β on mammosphere formation, cells were treated with TGF-β at the indicated dosages for 72 h before plating in undifferentiating sphere-culture conditions in the absence of TGF-β. When cells were transfected with plasmids, siRNAs or miRNA inhibitors, TGF-β was added at 6 h post transfection, and cells were treated for 3 days before sphere culture.

RNA extraction, RT and real time qPCR
This information can be found in the Supplementary Materials.

RNA immunoprecipitation assay
RNA immunoprecipitation was performed using a protocol modified from the chromatin immunoprecipitation assay described previously (Wang *et al*., 2005). In brief, cells were cross-linked for 10 min with 1% formaldehyde, lysed and sonicated (7 W, 10 s $\times$ 6). The lysates were cleared and subjected to immunoprecipitation with Smad2/3 or Drosha antibodies, or normal rabbit IgG (as a control). Precipitated RNA was isolated using TRIzol (Invitrogen) and subjected to RT and qPCR, as described above, using primers to detect pri-miR-181a-1 and the mature miR-181a. Samples precipitated with IgG were used as controls.

Western blot analysis
Preparation of cell lysates and western blot were carried out as described previously (Wang *et al*., 2007). Primary antibodies included the following: Oct4, Nanog, glyceraldehyde 3-phosphate dehydrogenase, Phospho(P)-HER2^{Y1248}, HER2, ATM, P-CHK2^{T68} and CHK2 (Cell Signaling, Danvers, MA, USA).

Immunofluorescence assay
Immunofluorescence assay was carried out as described previously (Wang *et al*., 2007). Fluorescent images were captured using a Princeton Instruments cooled CCD digital camera (Princeton Instruments, Trenton, NJ, USA) from a Zeiss upright LSM 510 2-Photon confocal microscope (Carl Zeiss MicroImaging, LLC, Thornwood, NY, USA) with a $\times$ 20/0.6 objection. Immunostaining of the mammospheres was performed in suspension, after fixation in 4% paraformaldehyde for 2 h followed by 20 min in cold methanol, following the same protocol as above. Primary antibodies include cytokeratin 5, cytokeratin 8/18 (Abcam, Cambridge, MA, USA), E-cadherin and N-cadherin (Santa Cruz Biotechnology, Santa Cruz, CA, USA). The fluorescent antibodies are Alexa Fluor 488-goat-α-rabbit IgG and Alexa Fluor 594-goat-α-mouse IgG (Invitrogen).

Cell transfection and RNA interference studies
DNA transfection was performed using Lipofectamine 2000 (Invitrogen) following the manufacturer's protocol, as described previously (Wang *et al*., 2006). The miRIDIAN miRNA hairpin inhibitors of miR-181a and miR-21 as well as the negative control were purchased from Dharmacon (Lafayette, CO, USA). Silencer siRNAs against human Smad4, ATM, CHEK2, BRCA1 and p53 as well as the AllStars negative control siRNA were purchased from Qiagen (Valencia, CA, USA). MiRNA inhibitors and siRNAs were transfected into cell lines using DharmaFECT Duo Transfection Reagent (Dharmacon) according to the manufacturer's procedures. In six-well plate format, a final concentration of 25 nM miRNA inhibitors or 100 nM siRNAs and 6 μl of DharmaFECT Duo Transfection Reagent mixed in 2 ml of serum-free medium were used for each transfection.

In vivo *tumorigenesis*
Six-week-old female NOD/SCID/IL2Rγ-null (NSG) mice were injected in the no. 4 mammary fat pad with 5×10^5 of MDA361/tetO-short hairpin RNA(ATM) cells, and divided into two groups (five mice per group) for treatment with Dox or control. For the group with Dox treatment, cells were pretreated *in vitro* with Dox (1 μg/ml) for 2 days before injection, and animals were administered 1 mg/ml Dox in 5% sucrose through drinking water starting at 2 days before cell injection. Mice were monitored for tumor formation twice weekly. Experimental protocols were approved by the Institutional Animal Care and Use Committee (IACUC) at City of Hope.

MiRNA microarray and ingenuity pathways analysis of predicted miRNA target genes
This information can be found in the Supplementary Materials.

Conflict of interest

The authors declare no conflict of interest.

Acknowledgements

This work was supported by NCI R00 CA125892 (SEW) and CBCRP 16IB-0081 (SEW). We thank Dr John J Rossi for kindly providing reagents, Dr Shiuan Chen and Dr Susan Kane for valuable comments, the Bioinformatics Core for professional service and colleagues in the Division of Tumor Cell Biology for enthusiastic support and discussion. Financial Support: NCI R00 CA125892 (SEW); CBCRP 16IB-0081 (SEW).

References

Ailles LE, Weissman IL. (2007). Cancer stem cells in solid tumors. *Curr Opin Biotechnol* **18**: 460–466.

Austen B, Skowronska A, Baker C, Powell JE, Gardiner A, Oscier D *et al*. (2007). Mutation status of the residual ATM allele is an important determinant of the cellular response to chemotherapy and survival in patients with chronic lymphocytic leukemia containing an 11q deletion. *J Clin Oncol* **25**: 5448–5457.

Charafe-Jauffret E, Ginestier C, Iovino F, Wicinski J, Cervera N, Finetti P *et al*. (2009). Breast cancer cell lines contain functional cancer stem cells with metastatic capacity and a distinct molecular signature. *Cancer Res* **69**: 1302–1313.

Cicalese A, Bonizzi G, Pasi CE, Faretta M, Ronzoni S, Giulini B *et al*. (2009). The tumor suppressor p53 regulates polarity of self-renewing divisions in mammary stem cells. *Cell* **138**: 1083–1095.

Cordenonsi M, Dupont S, Maretto S, Insinga A, Imbriano C, Piccolo S. (2003). Links between tumor suppressors: p53 is required for TGF-beta gene responses by cooperating with Smads. *Cell* **113**: 301–314.

Davis BN, Hilyard AC, Lagna G, Hata A. (2008). SMAD proteins control DROSHA-mediated microRNA maturation. *Nature* **454**: 56–61.

Derynck R, Zhang YE. (2003). Smad-dependent and Smad-independent pathways in TGF-beta family signalling. *Nature* **425**: 577–584.

Diederichs S, Haber DA. (2007). Dual role for argonautes in microRNA processing and posttranscriptional regulation of microRNA expression. *Cell* **131**: 1097–1108.

Dontu G. (2008). Breast cancer stem cell markers—the rocky road to clinical applications. *Breast Cancer Res* **10**: 110.

Dontu G, Abdallah WM, Foley JM, Jackson KW, Clarke MF, Kawamura MJ *et al*. (2003). *In vitro* propagation and transcriptional profiling of human mammary stem/progenitor cells. *Genes Dev* **17**: 1253–1270.

Dumont N, Arteaga CL. (2003). Targeting the TGF beta signaling network in human neoplasia. *Cancer Cell* **3**: 531–536.

Haidar MA, Kantarjian H, Manshouri T, Chang CY, O'Brien S, Freireich E *et al*. (2000). ATM gene deletion in patients with adult acute lymphoblastic leukemia. *Cancer* **88**: 1057–1062.

Ji J, Yamashita T, Budhu A, Forgues M, Jia HL, Li C *et al*. (2009). Identification of microRNA-181 by genome-wide screening as a critical player in EpCAM-positive hepatic cancer stem cells. *Hepatology* **50**: 472–480.

Kastan MB, Lim DS. (2000). The many substrates and functions of ATM. *Nat Rev Mol Cell Biol* **1**: 179–186.

Kong W, Yang H, He L, Zhao JJ, Coppola D, Dalton WS *et al*. (2008). MicroRNA-155 is regulated by the transforming growth factor beta/Smad pathway and contributes to epithelial cell plasticity by targeting RhoA. *Mol Cell Biol* **28**: 6773–6784.

Mani SA, Guo W, Liao MJ, Eaton EN, Ayyanan A, Zhou AY *et al*. (2008). The epithelial-mesenchymal transition generates cells with properties of stem cells. *Cell* **133**: 704–715.

Massague J. (2008). TGFbeta in cancer. *Cell* **134**: 215–230.

Pece S, Tosoni D, Confalonieri S, Mazzarol G, Vecchi M, Ronzoni S *et al*. (2010). Biological and molecular heterogeneity of breast cancers correlates with their cancer stem cell content. *Cell* **140**: 62–73.

Ren Y, Wu L, Frost AR, Grizzle W, Cao X, Wan M. (2009). Dual effects of TGF-beta on ERalpha-mediated estrogenic transcriptional activity in breast cancer. *Mol Cancer* **8**: 111.

Roberts AB, Wakefield LM. (2003). The two faces of transforming growth factor beta in carcinogenesis. *Proc Natl Acad Sci USA* **100**: 8621–8623.

Shipitsin M, Campbell LL, Argani P, Weremowicz S, Bloushtain-Qimron N, Yao J *et al*. (2007). Molecular definition of breast tumor heterogeneity. *Cancer Cell* **11**: 259–273.

Suzuki HI, Yamagata K, Sugimoto K, Iwamoto T, Kato S, Miyazono K. (2009). Modulation of microRNA processing by p53. *Nature* **460**: 529–533.

Topczewska JM, Postovit LM, Margaryan NV, Sam A, Hess AR, Wheaton WW *et al*. (2006). Embryonic and tumorigenic pathways converge via Nodal signaling: role in melanoma aggressiveness. *Nat Med* **12**: 925–932.

Tribius S, Pidel A, Casper D. (2001). ATM protein expression correlates with radioresistance in primary glioblastoma cells in culture. *Int J Radiat Oncol Biol Phys* **50**: 511–523.

Vallier L, Touboul T, Brown S, Cho C, Bilican B, Alexander M *et al*. (2009). Signaling pathways controlling pluripotency and early cell fate decisions of human induced pluripotent stem cells. *Stem Cells* **27**: 2655–2666.

Visvader JE, Lindeman GJ. (2008). Cancer stem cells in solid tumours: accumulating evidence and unresolved questions. *Nat Rev Cancer* **8**: 755–768.

Volinia S, Calin GA, Liu CG, Ambs S, Cimmino A, Petrocca F *et al*. (2006). A microRNA expression signature of human solid tumors defines cancer gene targets. *Proc Natl Acad Sci USA* **103**: 2257–2261.

Wang B, Hsu SH, Majumder S, Kutay H, Huang W, Jacob ST *et al*. (2010). TGFbeta-mediated upregulation of hepatic miR-181b promotes hepatocarcinogenesis by targeting TIMP3. *Oncogene* **29**: 1787–1797.

Wang SE, Narasanna A, Perez-Torres M, Xiang B, Wu FY, Yang S *et al*. (2006). HER2 kinase domain mutation results in constitutive phosphorylation and activation of HER2 and EGFR and resistance to EGFR tyrosine kinase inhibitors. *Cancer Cell* **10**: 25–38.

Wang SE, Narasanna A, Whitell CW, Wu FY, Friedman DB, Arteaga CL. (2007). Convergence of p53 and transforming growth factor beta (TGFbeta) signaling on activating expression of the tumor suppressor gene maspin in mammary epithelial cells. *J Biol Chem* **282**: 5661–5669.

Wang SE, Wu FY, Shin I, Qu S, Arteaga CL. (2005). Transforming growth factor \{beta\} (TGF-\{beta\})-Smad target gene protein tyrosine phosphatase receptor type kappa is required for TGF-\{beta\} function. *Mol Cell Biol* **25**: 4703–4715.

Watabe T, Miyazono K. (2009). Roles of TGF-beta family signaling in stem cell renewal and differentiation. *Cell Res* **19**: 103–115.

Supplementary Information accompanies the paper on the Oncogene website (http://www.nature.com/onc)